JOURNAL OF THEORETICAL AND APPLIED MECHANICS
50, 1, pp. 131-145, Warsaw 2012
50th anniversary of JTAM

A PARAMETER STUDY ON THE INFLUENCE OF FILLETS ON THE COMPRESSOR CASCADE PERFORMANCE

Robert Meyer, Sebastian Schulz, Karsten Liesner

German Aerospace Center DLR, Institute of Propulsion Technology – Department of Engine Acoustics, Berlin, Germany; e-mail: robert.meyer@dlr.de

Harald Passrucker, Roland Wunderer

MTU Aero Engines GmbH, Munich, Germany

In order to evaluate the influence of fillets in a high speed compressor cascade with an aspect ratio of $h/c = 1$ a parameter study has been performed. Fillets of different radii from 1 to 5 mm (2.5%c-12.5%c) between the side wall and stator vanes have been investigated at inlet Mach numbers of $\mathrm{M} = 0.5$ and $\mathrm{M} = 0.66$ and at a Reynolds number of $\mathrm{Re} = 5.6 \cdot 10^5$ based on the chord length. The heights of the fillets were chosen with regard to manufacturing aspects for blade integrated disks (Blisk). The measurements were accomplished with a total pressure rake combined with angle probes which provides information on total pressure loss, efficiency and outflow angle of the cascade. For comparison and estimation of the performance of the fillet equipped cascade a reference cascade without fillets was measured and the differences between the individual test cases will be shown in quantitative numbers and values as well as qualitative pictures. In the measurements for this paper a dependence between the fillet height and the total pressure loss coefficient became apparent.

Key words: fillet, compressor, blade, losses, secondary flow

Nomenclature

Geometric and flow quantities

M, Re	–	Mach and Reynolds number, [–]
c, h	–	vane chord length and vane height, [m]
$\dot{m}$	–	relative mass flow, [kg/(s·m^2)]
p_t, p	–	total and static pressure, [Pa]

t	–	blade pitch, [m]
u	–	peripheral coordinate, [m]
w	–	absolute speed, [m/s]
x, z	–	cascade axial and blade height coordinate, [m]
β	–	flow angle, [°]
$\Delta p/q, \zeta$	–	static pressure rise and total pressure loss coefficient, [–]

Subscripts

$1, 2$	–	inlet and outlet
av, t	–	averaged and total
BL	–	boundary layer
mw	–	mass weighted
P, S, W	–	profile, secondary flow and side wall, respectively

1. Introduction

The development of modern jet engines and stationary gas turbines is motivated by increasing engine performance and efficiency and by reducing costs, weight and emission. In order to cut down on weight in the axial compressor, the number of stages must be minimised without changing the overall pressure ratio. Consequently, the stage pressure ratio must be increased. As the stage pressure rise depends on circumferential velocity and flow deflection, low aspect ratio designed blades need to be used to allow a larger static pressure rise per stage. In order to ensure mechanical strength at high tip speeds, low aspect ratio designed rotors are manufactured as Blisks with lager fillet radii than conventional rotor designs.

The addition of fillets or the increase of the fillet radius has an impact on the aerodynamic performance of the cascade because it influences the interaction between the end wall and blade boundary layers. DeBruge finds in a theoretical investigation (DeBruge, 1980) fillets able to remove 3D corner flow due to a thinner boundary layer in the corner region with less affinity to separate. Calvert and Ginder (1999) stated that for aerodynamical reasons in a transsonic compressor the fillet radius should be larger than it is needed mechanically. However, experimental investigations in Curlett (1991) show that for Controlled Diffusion Airfoil (CDA) the secondary flow and losses increase when using fillets. But contrary effects were shown in Curlett (1991) for Double Circular Arc (DCA) blades. For higher incidence angles the losses decreased. A coherence between the incidence angle and fillets were found in Hoeger *et al.* (2006), too. There fillets were found to remove corner stall for high incidence

angles. Kuegler *et al.* (2008) showed in a numerical investigation of a multistage compressor a higher throttling range for the fillet equipped compressor due to reduced corner stall. A fillet vortex which turned in the opposite direction to the horse-shoe vortex were detected numerically in Hoeger *et al.* (2002). This vortex transports high energy fluid to the suction surface of the blade and thereby prevents the separation of the boundary layer.

The present paper deals with the influence of increasing fillet radii on the high speed compressor cascade performance and secondary flow. An experimental investigation on a plain, transsonic compressor cascade has been performed.

2. Experimental setup

2.1. Wind tunnel and test section

All experiments are carried out at the high speed stator cascade wind tunnel of the German Aerospace Center (DLR) in Berlin. The wind tunnel air is driven by a radial compressor powered by an AC motor and supplied to the test section via a silencer, a diffusor, a settling chamber and a nozzle with a contraction ratio of 1:218. Mach numbers of 0.7 and Reynolds numbers of up to $0.65 \cdot 10^6$ can be obtained. The test section of the wind tunnel (Fig. 1) has a rectangular cross section of 40 mm width and 82 mm height at the cascade inlet. It provides independent boundary layer adjustment options of all four side walls.

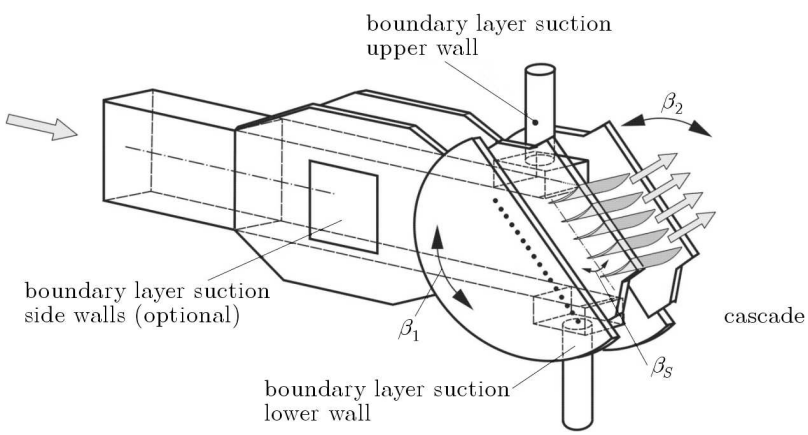

Fig. 1. Sketch of the test section

The upper and lower boundary layers are sucked to obtain a periodic flow in the compressor cascade. By monitoring the static pressure in the pitchwise direction in the cascade inlet plane the periodicity is ensured. The side wall boundary layer can be set from 3-12 mm (7.5%c-30%c) by varying the inlet length. By boundary layer suction, the thickness can be decreased to less than 2 mm (5%c). The boundary layer parameters are measured in a boundary layer rake upstream of the cascade. In order to determine the whole working range of the compressor cascade, the inlet angle β_1 can be adjusted geometrically from 122° to 146°.

2.2. Data acquisition

A rake with 26 pitot tubes for total pressure measurement, four Conrad angle probes for outflow angle determination, and a static pressure probe is used for the wake measurements. The wake rake is arranged in the blade height direction z and can be traversed in the circumferential direction u. In order to minimise the influence of the upper and lower channel side wall only the middle blade is investigated from $u = -t/2$ to $u = t/2$. Coordinates are shown in Fig. 2. The measurement plane is located 16 mm (40% chord length) downstream of the cascade outlet.

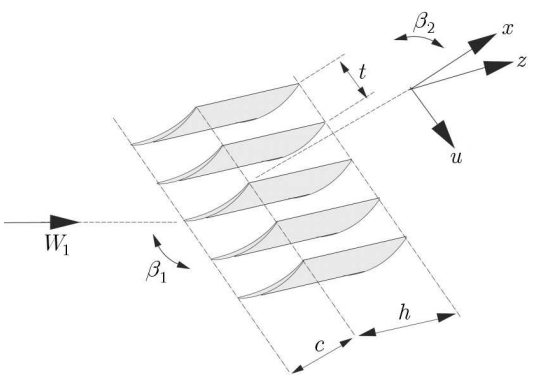

Fig. 2. Coordinates in the test section

Due to the use of high accurate pressure transducers and arithmetical averaging over a high number of pressure values, reproducibility with deviations of less than ±0.2% of the loss coefficient is ensured. A detailed description of the wind tunnel and measurement procedures can be found in Liesner *et al.* (2008).

2.3. Cascade geometry and test conditions

The plain cascade consist of five airfoils of the NACA65 family which are taken at a section of 10% of the vane height of the axial compressor of the University of Darmstadt. The blades are fixed at the side walls without gaps. The aspect ratio is $h/c = 1.0$ with a chord length of $c = 40\,\text{mm}$. The flow is deflected by the blades about $\Delta\beta = \beta_1 - \beta_2 = 37.7°$. According to the aerodynamic design condition, the inlet angle β_1 is set to 132°. The reference case without fillets and three cascades with different fillet radii (1 mm, 3 mm and 5 mm, respectively) were investigated at inlet Mach numbers of $\mathrm{M} = 0.5$ and $\mathrm{M} = 0.66$. All relevant cascade data are given in Table 1.

Table 1. Geometric and aerodynamic parameters of the cascade

Compressor cascade	Values	Units
chord length c	40	[mm]
pitch t/c	0.55	[–]
aspect ratio h/c	1	[–]
inlet flow angle β_1	132	[°]
stagger angle β_s	105.2	[°]
flow deflection $\Delta\beta$	37.7	[°]
outlet flow angle β_2	94.3	[°]
Inlet Mach numbers M	0.5 and 0.66	[–]
Reynolds numbers Re	433025 and 561981	[–]
boundary layer thickness δ_{99}	3.4 and 3.1	[mm]

The heights of the fillets were chosen with regard to manufacturing aspects for Blisks. The highest point on the stagnation line of the fillet with 3 mm radius is slightly under the height of the boundary layer thickness of the incoming flow. All fillets offer a concave shape, blend both to the end wall and the blade, and encircle the blades completely (Fig. 3). A rubber modelling material was used to produce the fillets because of its smooth surface and shaping ability.

For the comparison of different cascades, the total pressure loss coefficient is used. It is calculated in the usual way

$$\zeta_t(u,z) = \frac{p_{t_1}(u,z) - p_{t_2}(u,z)}{q_1}$$

In order to give valuable information on the distribution of the loss coefficient on the cascade behaviour, the total pressure loss coefficient is weighted

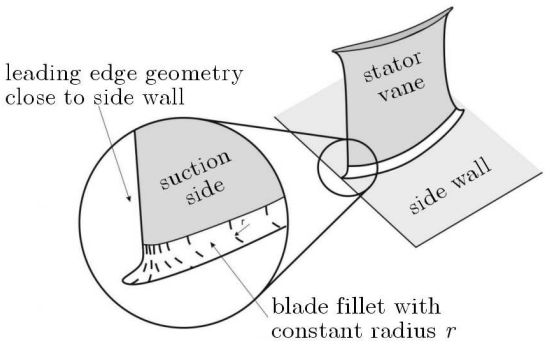

Fig. 3. Fillet geometry and shape

by a mass-flow averaging. The mass flow is the product of density, channel area and flow velocity. The averaged total pressure loss coefficient is calculated in the following manner

$$\zeta_{t_{mw}} = \frac{\zeta_t(u,z)\ \dot{m}(u,z)}{\dot{m}}$$

3. Results

The cascades are evaluated on the basis of three different flow parameters, as there are the flow deflection $\Delta\beta$, the static pressure rise $\Delta p/q$ and the overall total pressure loss coefficient ζ_t. The total pressure loss coefficient ζ_t is subdivided into airfoil losses ζ_P and side wall losses ζ_W. The airfoil losses are the amount of losses in the half span of the blade. It is assumed there is no more side wall influence measurable. Side wall losses are the sum of inlet boundary layer losses ζ_{BL} and secondary flow losses ζ_S.

3.1. Results at inlet Mach number M=0.66

In order to characterise the influence of the fillets on the flow, the flow parameters from the fillet equipped cascades are compared to the reference cases. The result of the reference cascade without fillets at the inlet Mach number $\mathrm{M} = 0.66$ is shown in Fig. 4.

The upper part of Fig. 4 contains the distribution of the mass flow averaged local total pressure coefficient $\zeta(u,z)$ from $u = -t/2$ to $u = t/2$. Zero marks the trailing edge of the blade. Resulting from secondary flow and flow separation, two distinct vorticies can be identified. The vane wake pressure loss is

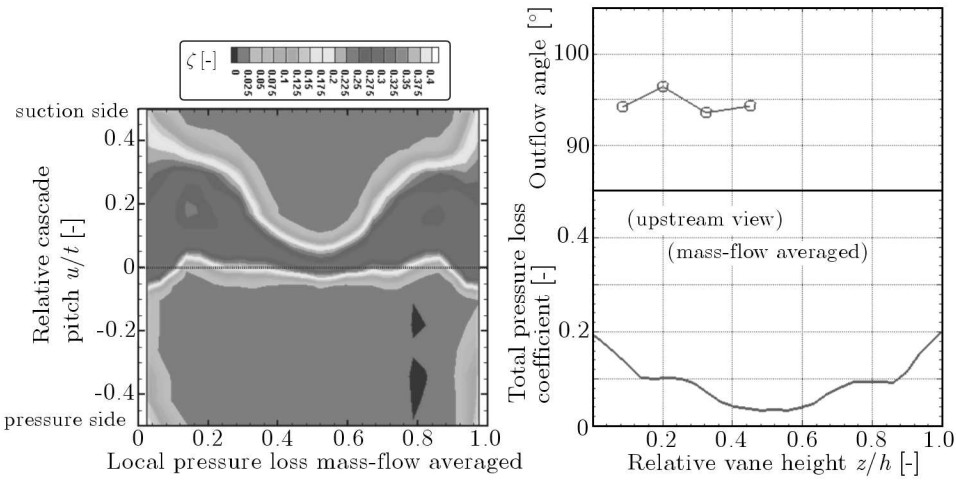

Fig. 4. Reference case; M = 0.66, Re = 561981

visible in the symmetry plane of the cascade. The middle part of Fig. 4 shows the integral flow outlet angle β_2 at four discret spanwise positions. The lower the outflow angle is, the higher is the flow deflection by the stator cascade. The integral averaged total pressure loss coefficient along the vane height z is shown in the lower part of Fig. 4. The influence of the side wall boundary layer is visible on the left and right side, the plateaus at $z/h = 0.2$ and 0.8 mark the losses due the vorticies mentioned above. In the symmetry plane of the cascade, again only the vane wake pressure loss is visible. In Table 2, the flow parameters of the different cascades and a comparison between the fillet and reference cases are given.

Table 2. Flow parameters and divergence at M = 0.66

		$\Delta p/q$	ζ_t	ζ_P	ζ_W
Reference		0.355	0.091	0.033	0.058
1 mm	value	0.366	0.092	0.035	0.057
	divergence	3.2%	1.8%	8.0%	−1.7%
3 mm	value	0.363	0.095	0.038	0.057
	divergence	2.3%	4.8%	16.9%	−1.9%
5 mm	value	0.333	0.103	0.041	0.063
	divergence	−6.2%	14.3%	25.2%	8.1%

In order to compare the reference and the fillet equipped cascades properly, comparison layouts have been developed to show the differences in a 2D layout. In Fig. 5, the comparison between the reference and 1 mm fillet cascade is shown, red to magenta colours indicate regions of loss increase, yellow to green indicate regions of loss decrease. The slight asymmetry may result from the manufacturing procedure where handcraft is used to form the fillets. This does not affect the general statement of the measurement.

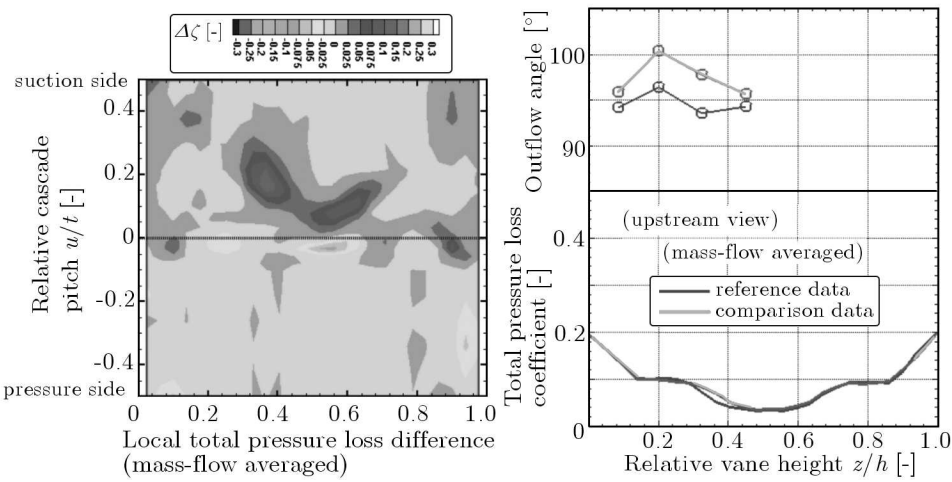

Fig. 5. Comparison layout: 1 mm fillet with reference; M = 0.66, Re = 561981

In comparison to the reference cascade at the inlet Mach number M = 0.66, the total pressure loss coefficient distribution of the cascade with 1 mm fillets shows slightly increased losses at the outer edge of the vorticies next to the symmetry plane. The increase of the total pressure loss coefficient is about 1.8% (see Table 2) with an increase of 8% for the profile losses ζ_P and a decrease of 1.7% for the wall losses ζ_W. The flow is 1.4° less deflected at $z/h = 0.45$ as in the reference case. However, the change of the flow deflection is more significant in the region of the vorticies than in the symmetry plane of the cascade. Despite the increase of the total pressure loss coefficient, the static pressure rise increases about 3.2%.

The increase of the static pressure rise in the 3 mm fillet case is not as distinct as for the 1 mm fillet. It rises about 2.3%. The total pressure loss coefficient increases about 4.8%. It indicates higher losses in the middle of the passage in the same way as in the latter case but more distinct (Fig. 6). In addition, a rise of losses can be found around the trailing edge at z/h = 0-0.2 and 0.8-1. They are identifiable in the 1 mm case as well. The change of flow

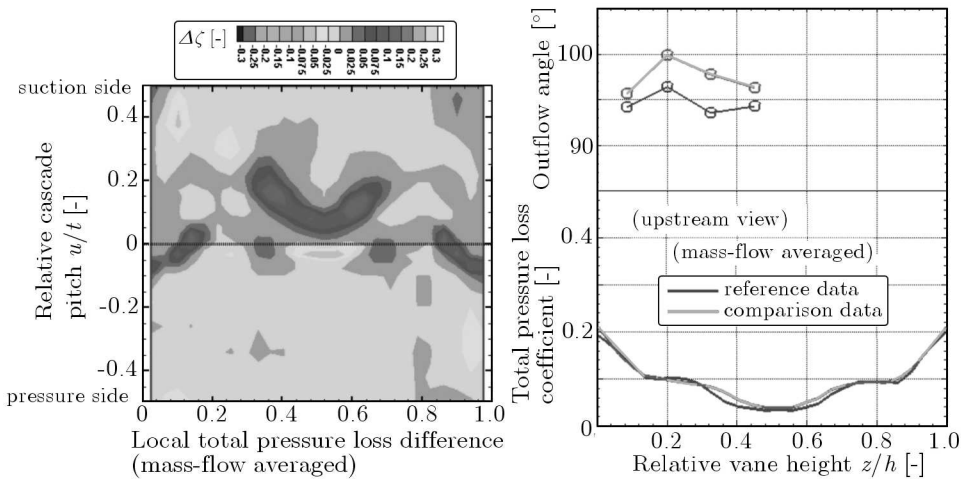

Fig. 6. Comparison layout: 3 mm fillet with reference; M = 0.66, Re = 561981

deflection shows the same characteristics as the 1 mm fillet case with a slight change at the side wall and symmetry plane and higher distinction compared to the reference in the vortex region.

By contrast, the flow deflection of the 5 mm fillet case increases at the side wall, and in the symmetry plane it nearly did not change. The total pressure loss coefficient increases about 14.3%, the profile and wall loss about 25.2% and 8.1%, respectively. It shows a similar distribution as the results previously discussed. There is a decrease of the static pressure rise about 6.2% for this case.

In summary, the results at M = 0.66 show a dependence between the fillet height, the total pressure loss coefficient and the static pressure rise. The bigger the fillet radii, the higher the losses. Contrary to that the static pressure rise increases for 1 mm fillet more than for 3 mm fillet and finally decreases for the 5 mm fillet case. The loss distribution is shifted to the symmetry plane with a smaller pitchwise distribution next to the side walls compared to the reference. The change of flow deflection is largest for 3 mm fillet case and lowest for the 5 mm fillet equipped cascade. However, the flow deflection is highest for the reference cascade without fillets.

3.2. Results at inlet Mach number M=0.5

The results for measurements at inlet Mach number M = 0.5 show similar characteristics as the results presented above. The amount of losses in the flow field at M = 0.5 are smaller than at higher Mach numbers but the

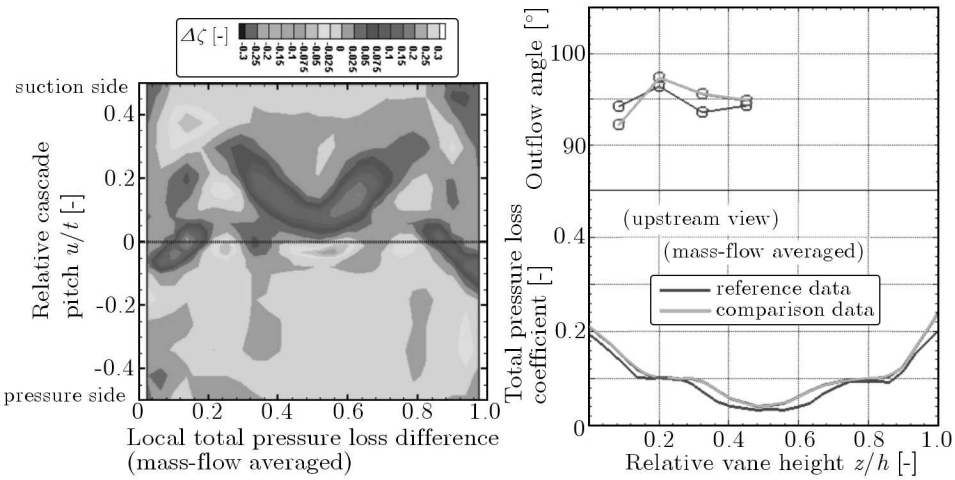

Fig. 7. Comparison layout: 5 mm fillet with reference; M = 0.66, Re = 561981

distributions are the same. For the 1 mm fillet case at M = 0.5 any changes are hardly recognisable. Actually, the total pressure loss coefficient nearly stays constant with the static pressure rise increasing by 3.1%. At the side walls the flow is less deflected as in the reference but the vortex region shows no identifiable difference. A summary of all flow paramteres and a comparsion with the reference is given in Table 3.

Table 3. Flow parameters and divergence at M = 0.5

		$\Delta p/q$	ζ_t	ζ_P	ζ_W
Reference		0.342	0.084	0.030	0.054
1 mm	value	0.361	0.084	0.030	0.054
	divergence	3.1%	−0.1%	1.0%	−0.7%
3 mm	value	0.352	0.087	0.034	0.053
	divergence	2.7%	4.3%	15.9%	−2%
5 mm	value	0.323	0.093	0.035	0.058
	divergence	−7.7%	11.2%	19.3%	6.8%

In the distribution of the total pressure loss coefficient of 3 mm and 5 mm cases at M = 0.5 is an increase of losses in the same regions recognisable as there were at M = 0.66: in the symmetry plane at the outer edge of the vorticies and around the trailing edge at z/h = 0-0.2 and 0.8-1. At both Mach numbers the shift of the loss distribution to the symmetry plane and the decrease of the pitchwise losses next to the side walls are recognisable.

The total pressure loss coefficient increases about 4.3% for the 3 mm and 11.2% for the 5 mm case, respectively. There is an increase of the static pressure rise for the 3 mm fillet equipped cascade about 2.7%, whereas there is a decrease of about 7.7% for the 5 mm fillet case. This may be due to the reduction of the passage area that works as a nozzle and accelerates the flow slightly. The change of flow deflection is, as it were for $M = 0.66$, lowest for 5 mm fillets and highest for the 3 mm fillet case. At $M = 0.5$, the flow deflection is highest for the reference cascade as well – just as the losses grow with the fillet radii.

4. Discussion

The 3D flow in a compressor cascade causes the total pressure loss coefficient distributions observable in Fig. 4. The inlet side wall boundary layer at vane leading edge rolls up to form the so called horseshoe vortex (Fig. 8). Due to increasing streamline curvature in the compressor cascade, the side wall boundary layer is superimposed by a pressure gradient transverse to the flow direction. A cross flow from the pressure to suction side inside the wall boundary layer emerges, feeding the horseshoe vortex with fluid and energy to build up the passage vortex. The interaction of the side wall and vane boundary layer with the passage vortex causes the corner vortex which rotates in the opposite direction as the passage vortex. Behind the vane, wake flow recirculation occurs due to pressure compensation.

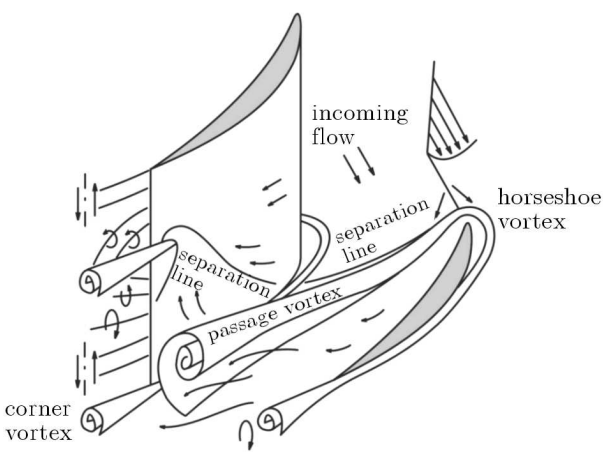

Fig. 8. 3D flow through an axial compressor cascade according to Kang (Kang and Hirsch, 1991)

There is an increase of total pressure loss at z/h = 0-0.2 and 0.8-1 and $u/t = \pm 0.05$ which can be identified in Figs. 5, 6 and 7. This is possibly generated by the wake loss of the fillets. With the placement of the fillets into the flow, an additional form drag occurs which induces wake losses. Of course, the wake loss of the fillet grows with growing fillet radius. In Figs. 5, 6 and 7, an increase of losses next to the symmetry plane can be recognised. With growing radii of the fillets, this effect increases. Due to the displacement effect of the fillets, the 3D flow structures are shifted to the symmetry plane, and by that the losses in the middle of the passage increase with a slight decrease in the side wall region. Consequently, this effect describes a loss reallocation with only a slight increase of losses. This is supported by the development of wall losses ζ_W and profile losses ζ_p shown in Tables 2 and 3. For 1 mm and 3 mm fillets, the wall losses decrease with an increase of profile losses. Only for 5 mm fillet profile, the wall losses increase. That can be explained with the high fillet wake losses due to the large fillet radius. Furthermore, the 5 mm fillet does not only effect the corner boundary layer but the undisturbed flow as well, which causes an increase of losses.

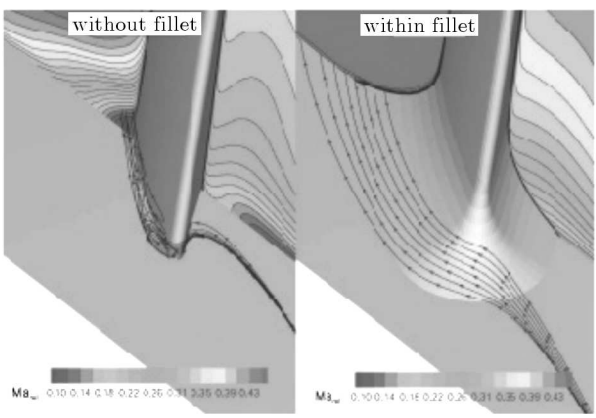

Fig. 9. Streamline at the leading edge (Kuegeler *et al.*, 2008)

With a fillet added to the vane, the corner boundary layer is removed but the fluid is guided from the vane to the side wall (Fig. 9), and by that more high energy fluid is added to the cross flow from the pressure to suction side producing an increase of vorticity of the passage vortex. Consequently, the axial velocity decreases resulting in a static pressure rise which can be observed in the 1 mm and 3 mm fillet cases. For increasing fillet radii, this effect is overruled by the distinct displacement effect for this case. Due to

the decreased flow cross section, the axial velocity accelerates and causes a static pressure drop in order to meet mass conservation. As the 1 mm fillet is nearly as high as the displacement thickness of the boundary layer, there is no additional reduction of the flow cross section, and therefore no axial velocity acceleration. The 1 mm fillet case offers the highest static pressure rise of the investigated cascades. For the 3 mm fillet case, the influence of the reduced flow cross section becomes more obvious as a result of a smaller static pressure rise. A static pressure drop is provided by the 5 mm fillet case where the flow cross section reduction completely overrules the increased vorticity of the passage vortex caused by increased cross flow.

On the basis of the integral flow outlet angle β_2 distribution (Figs. 5, 6 and 7) in the spanwise direction, it is recognisable that the addition of fillets into the flow reduces flow deflection due to the described secondary flow shift. The influence of the corner vortex becomes apparent. In the reference case, the angle probes were not able to measure the corner vortex as the displacement between the probes and the side wall were too big. In the fillet cases, the corner vortex is shifted in the spanwise direction and therefore influences the measurable flow deflection. The corner vortex produces an increasing flow deflection in the side wall region at $z/h = 0.1$ (Fig. 7) and the counter rotating passage vortex gives a reduced flow deflection at $z/h = 0.32$. For smaller fillets the second (at $z/h = 0.21$) and third measurement point (at $z/h = 0.32$) seem to rotate around the first (at $z/h = 0.1$) indicating a reduced flow deflection in this region (Figs. 5 and 6). The corner vortex hardly influences the measurements and therefore only a slightly increasing flow deflection at the first measurement point is identifiable. The shift of the passage vortex produces a downwash and therefore the flow is less deflected at the second and third measurement point compared to the reference.

5. Conclusions

A plain compressor cascade with fillet radius of 1 mm, 3 mm and 5 mm, respectively, has been investigated at the high speed stator cascade wind tunnel of the German Aerospace Center (DLR) in Berlin. The measurements show that the losses increase with growing fillet radii. This effect is found for both measured Mach numbers, but the higher the Mach number is, the higher are the losses. On the suction side, the 3D flow structures of the secondary flow are shifted to the symmetry plane due to the displacement effect of the fillets

producing higher losses in the middle of the passage but less in the side wall region. On the pressure side, the additional drag of the fillets produces additional losses in the corner region. The corner losses present the main part of increasing losses due to fillets. A static pressure rise could be observed for fillets smaller than the boundary layer thickness. An increased cross flow induces higher vorticity of the passage vortex and by that decelerates the axial velocity resulting in a static pressure rise. For lager fillets, the displacement effect overrules the increasing vorticity producing a static pressure drop due to mass conservation.

References

1. Calvert W.J., Ginder R.B., 1999, Transonic fan and compressor design, *Proceedings of the Institution of Mechanical Engineers, Part C: Journal of Mechanical Engineering Science*, **213**, 5, 419-436

2. Curlett B.P., 1999, *The Aerodynamic Effect of Fillet Radius in a Low Speed Compressor Cascade*, National Aeronautics and Space Administration, Lewis Research Center, USE, NASA-TM-105347

3. DeBruge L.L., 1980, The aerodynamic significance of fillet geometry in turbocompressor blade rows, *ASME Journal of Engineering for Power*, **102**, 984-993

4. Hoeger M., Baier R.-D., Engbert M., Mueller R., 2006, *Impact of a Fillet on Diffusing Endwall Flow Structure*, ISROMAC 2006-057

5. Hoeger M., Schmidt-Eisenlohr U., Gomez S., Mueller R., Sauer H., 2002, Numerical simulation of the influence of a bulb and a fillet on the secondary flow in a compressor cascade, *TASK Quatery*, **6**, 1, 25-57

6. Kang S., Hirsch Ch., 1991, Three dimensional flow in compressor cascades, *ASME Paper No. 91-GT-114*, Orlando, FL, USA

7. Kuegeler E., Nuernberger D., Weber A., Engel K., 2008, Influence of blade fillets on the performance of a 15 stage gas turbine compressor, *Proccedings of ASME Turbo Expo 2008*, GT2008-50748

8. Liesner K., Meyer R., Hergt A., 2008, Experimental setup for detailed secondary flow investigation by two-dimensional measurement of total pressure loss coefficients in compressor cascades, *XIX Symposium on Measurement Techniques in Turbomachinery*

Badania parametryczne wpływu powierzchni przejściowej łopatek na wydajność sprężarki kaskadowej

Streszczenie

W celu oszacowania wpływu powierzchni przejściowej łopatek w wysokoobrotowych sprężarkach kaskadowych o współczynniku kształtu $h/c = 1$ na ich wydajność w pracy przeprowadzono analizę parametryczną układu. Profile przejściowe o promieniach zaokrągleń od 1 do 5 mm (2.5%c-12.5%c) pomiędzy powierzchnią osadzenia a łopatką kierownicy badano dla prędkości napływu 0.50-0.66 M i liczbie Reynoldsa $\mathrm{Re} = 5.6 \cdot 10^5$ przy zadanej długości cięciwy łopatki. Wysokość profilu przejściowego dobrano ze względów technologicznych typowych dla dysków zintegrowanych z łopatkami. Pomiary dokonano za pomocą czujników ciśnienia i próbników kątowych, co pozwoliło na zgromadzenie informacji o całkowitych stratach ciśnienia, sprawności i wartości kąta odpływu z kaskady. Dla celów porównawczych i wyznaczenia wydajności sprężarki przeprowadzono pomiary w kaskadzie referencyjnej pozbawionej powierzchni przejściowych. Różnice dla poszczególnych testów pokazano ilościowo na wartościach konkretnych parametrów i jakościowo na odpowiednich rysunkach. Pomiary wykazały wyraźną zależność pomiędzy wysokością profilu przejściowego i współczynnikiem całkowitych strat ciśnienia.

Manuscript received September 22, 2010; accepted for print April 11, 2011